A new constitutive model for natural deposit clays: development and verification

Weiyi Wang[1], *Wenxuan* Zhu[1], *Guanlin* Ye[1], *Feng* Zhang[2], and *Hehua* Zhu[2]

[1] Department of Civil Engineering, Shanghai Jiao Tong University, Shanghai, China.
[2] Department of Geotechnical Engineering, Tongji University, Shangha, China.

1 Introduction

Shanghai clay, in particular, exhibits highly complex mechanical characteristics, including overconsolidation, structure, anisotropy, and significant effects of small-strain stiffness (SSS). Accurately capturing these properties and integrating them within a single constitutive framework is a key challenge for improving the precision of numerical analyses in soft soil engineering.

In this paper, Shanghai Model (SHM), a sophisticated constitutive model that incorporates overconsolidation, structure, anisotropy, and SSS of Shanghai clays is proposed in a unified way. Based on the experimental data on Shanghai clays, the predictive capabilities of SHM were validated in terms of structure, overconsolidation, anisotropy and SSS.

2 Shanghai Model and parameter determination

2.1 Derivation of Shanghai Model

The new model, named Shanghai Model (SHM), is developed within the framework of critical state soil mechanics, incorporating the fundamental concepts of anisotropy [1], subloading [2], and superloading yield surface [3]. A schematic diagram illustrating three geometrically similar yield surfaces is presented in Figure 1. The evolution rule for degree of structure R^*, overconsolidation R, and anisotropic tensor β_{ij} follows established rules (details in previous works [4, 5]). Regarding SSS characteristics, the shear modulus degradation was characterized using the tangent stiffness model [6, 7] as Equation (1) and Equation (2).

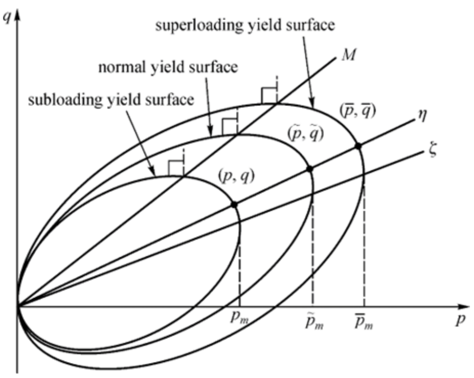

Figure 1. Subloading, normal and superloading yield surfaces in *p*-*q* plane [4].

$$G = \begin{cases} \dfrac{G_0}{(1+\alpha\gamma/\gamma_{0.7})^2} & \gamma < \gamma_c \\ \dfrac{E}{2(1+\nu)} & \gamma \geq \gamma_c \end{cases} \tag{1}$$

$$E = \frac{3(1-2\nu)(1+e_0)}{\kappa} p \tag{2}$$

2.2 Calibration of parameters

SHM consists of a total of 9 parameters for large-strain range and 2 parameters for SSS, as well as 3 initial state variables. Among which, 5 parameters (e_0, v, λ, κ, and M) are the same with the Cam-clay model, including: reference void ratio e_0, Poisson's ratio v, critical state shear ratio M, compression index λ, swelling index κ. Another 4 parameters control the evolution of soil properties: degradation parameter of overconsolidation m, degradation parameter of structure a, evolution parameter of anisotropy b_r, parameter of plastic strain ratio A.

* Corresponding author: ygl@sjtu.edu.cn

The parameter calibration for SHM follows a systematic, sequential procedure.

1. The five fundamental material parameters (e_0, v, λ, κ, and M) are identical to those in the Cam Clay model. These parameters can be directly calibrated using data from standard consolidation and triaxial tests on remolded soil samples.
2. The parameters governing the evolution of the three state variables (m, a, b_r) and parameter A are calibrated by data from triaxial tests conducted on undisturbed (natural) soil samples reflecting their *in-situ* state.
3. SSS parameters (G_0, $\gamma_{0.7}$) are determined using high-precision triaxial tests equipped with LVDTs (Local Vertical Displacement Transducers).
4. Initial state variables (R_0, R_0^*, ζ_0) are not material constants; they reflect the soil's specific *in-situ* condition.

Following the above calibration steps, the obtained material parameters and initial state variables for Shanghai clays are listed in Table 1 and Table 2.

Table 1. Material parameters and initial states of Shanghai clays.

Layer	e_0	v	λ	κ	M	m	a	b_r	p_c (kPa)	R_0^*	ζ_0
Layer 2	0.82	0.3	0.1167	0.0257	1.2	1	0.1	1.2	88	1	0
Layer 3	0.78	0.3	0.0623	0.0096	1.35	1	0.2	-	66.5	0.8	0
Layer 4	0.74	0.3	0.1713	0.0349	1.25	2	0.3	0.3	88	0.1	0
Layer 5_{-1}	0.92	0.3	0.1111	0.0174	1.3	0.1	0.5	0.4	198	0.6	0
Layer 5_{-2}	0.87	0.3	0.1075	0.0174	1.45	0.3	0.8	2.0	192	0.6	0
Layer 6	0.63	0.3	0.0648	0.0111	1.25	0.1	1	0.2	460	1	0

[a] In isotopic consolidated tests, $\boldsymbol{\zeta_0} = 0$, b_r=0.

Table 2. SSS parameters and initial conditions of Shanghai clays for CK_0U tests.

Layer	OCR	R_0*	*TC*					*TE*				
			G_0	$\gamma_{0.7}$	p_0	ζ_0	K_0	G_0	$\gamma_{0.7}$	p_0	ζ_0	K_0
Layer 2	4.5	1	27.0 E3	2.5 E-4	22	0.1	0.625	8.6 E3	4.1 E-4	17	0.1	0.625
Layer 4	1.0	0.3	22.5 E3	2.8 E-4	98	**0.5**	0.625	17.7 E3	3.9 E-4	59	**0.1**	0.6
Layer 5_{-1}	1.5	1.0	36.2 E3	1.0 E-4	132	0.54	0.6	30.2 E3	4.0 E-4	110	0.3	0.576
Layer 5_{-2}	1.4	0.8	65 E3	1.2 E-4	192	0.54	0.6	100 E3	2.2 E-4	186	0.54	0.6
Layer 6	2.5	1.0	80 E3	1.4 E-4	208	0.54	0.6	110 E3	2.3 E-4	213	0.54	0.6

[a] For layer 2 and TE of Layer 4&5_{-1}, $\boldsymbol{\zeta_0} \neq \eta$, having better fitting effect.

3 Validation of Shanghai Model by laboratory tests

Laboratory tests were conducted on Shanghai clays from Layers 2 to 8, including oedometer, CIU, CK_0UC, and CK_0UE tests. The performance of SHM is validated by those series of laboratory tests.

3.1 Simulation of structured clay

Layer 4 is a structured, highly sensitive marine clay ($S_t \approx 5{\sim}10$) deposited in a littoral environment. In oedometer tests, it exhibits high compressibility with a distinct yield point at the pre-consolidation pressure and rapid structure degradation under high stress. In undrained shear, the soil shows strong confining-pressure dependence and pronounced strain-softening. SHM captures both behaviors using a consistent set of parameters. The model reveals a two-stage mechanism: overconsolidation dissipates rapidly at small strains, dominating the initial dilative response; subsequently, progressive structure degradation dominates, inducing negative dilatancy and strain-softening. This sequential control explains the reverse-type stress path observed at low confining stress, where the stress path first rises along the CSL and then turns downward—a feature successfully reproduced by SHM.

3.2 Simulation of overconsolidated clay

As for overconsolidated clay, in oedometer tests, it exhibits typical behavior: high stiffness with a flat compression curve before the pre-consolidation pressure, followed by a sharp slope converging to the normal consolidation line (NCL) after yielding. Although the compression curve shape resembles that of structured clay, the underlying mechanism differs—overconsolidated behavior is governed by stress history memory rather than structural bonding. SHM captures this response: for soils with OCR = 1.5 and 16, the simulations match the experimental curves, showing that higher OCR leads to more rapid convergence toward NCL upon loading. In undrained shear, overconsolidated clay exhibits dilatancy, with the effect more pronounced at lower confining stresses. The mechanism is governed by overconsolidation dissipation: at small strains, positive pore pressure develops; as shearing progresses, overconsolidation dissipates, inducing dilatancy—pore pressure decreases, mean effective stress increases, and the stress path moves upward-right. SHM successfully reproduces this behavior across different confining stresses.

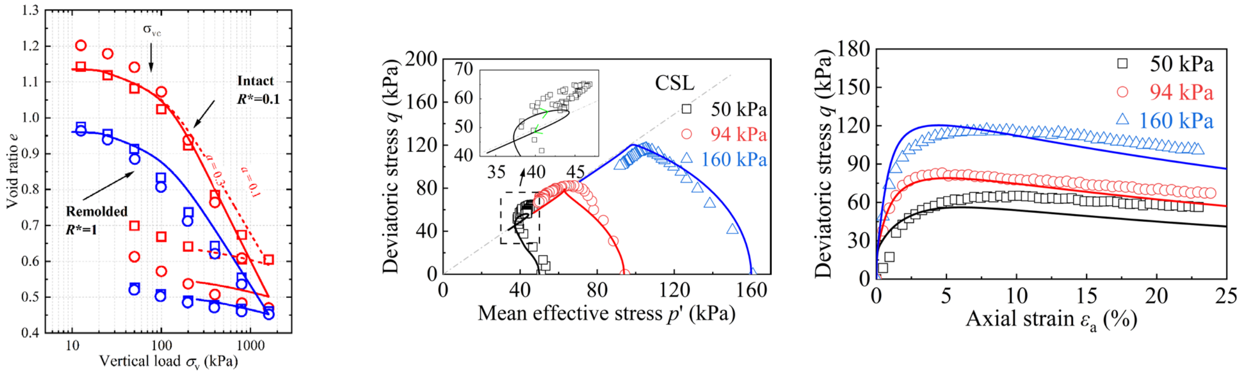

(a) (b) (c)

Figure 2. Test and simulation results of tests on structured clay: (a) Oedometer test of structured clay, (b) Effective stress path of CIU tests and (c) q–ε_a curves of CIU tests.

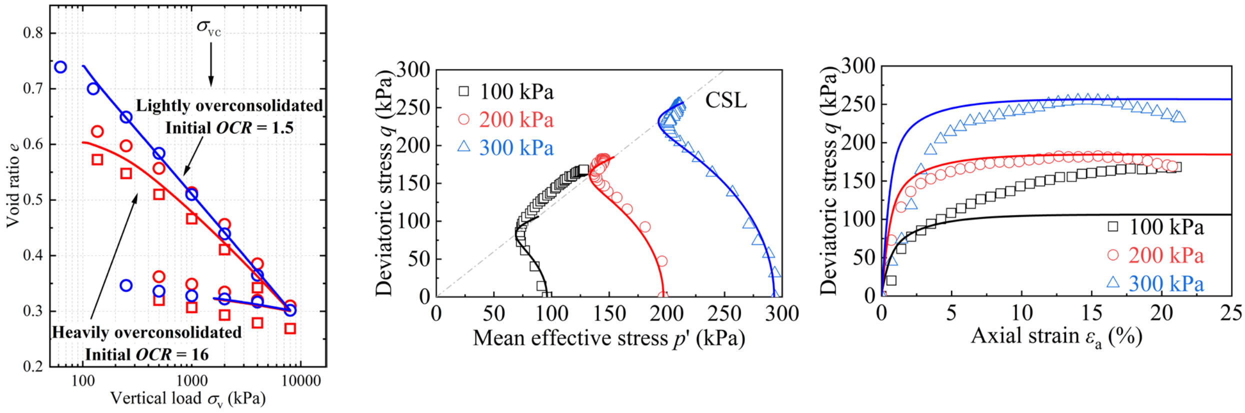

(a) (b) (c)

Figure 3. Test and simulation results of tests on overconsolidated clay: (a) Oedometer test of structured clay, (b) Effective stress path of CIU tests and (c) q–ε_a curves of CIU tests.

3.3 Simulation of soil anisotropy

Shanghai clays exhibit significant anisotropy in both strength and stiffness. CK_0U tests reveal that the stress paths of different layers vary considerably: overconsolidated Layer 2 shows symmetric strain-hardening paths, structured Layer 4 displays symmetric strain-softening, while Layers 5 and 6 exhibit asymmetric paths about the p'-axis, indicating a rotated (anisotropic) yield surface. This anisotropy is further evidenced by lower M_f values in extension than compression, and higher peak strength in TC than TE.

Interestingly, stiffness anisotropy shows an opposite trend—normalized secant stiffness G/p' is higher in TE than TC at small strains. SHM captures these behaviors by introducing initial anisotropy ζ_0. For K_0-consolidated Layer 6, simulations with ζ_0=0.54 successfully reproduce the asymmetric stress path and the complex EPWP evolution in TE tests: negative at ε_a<0.2%, positive at 0.2~5%, and negative again beyond 5%. This three-stage response is explained by the ESP's position relative to the total stress path (TSP). While SHM accurately simulates large-strain response with unified parameters, small-strain parameters (G_0, $\gamma_{0.7}$) currently require separate calibration for TC and TE in most layers (except structured Layer 4), reflecting the inherent anisotropy and calling for future development of a unified anisotropic SSS model.

3.4 Simulation of small strain stiffness (SSS)

Shanghai clays exhibit significant small-strain stiffness (SSS) behavior. As shown in Figure 4, the implementation of the SSS module in SHM enables accurate capture of the nonlinear stiffness degradation within the small-strain range (ε_a < 1%). Below the threshold strain γ_c, conventional elastoplastic methods substantially underestimate stiffness, while the proposed SSS formulation (Equation (2)) effectively bridges this gap, yielding predictions that closely match experimental measurements. Importantly, the incorporation of SSS does not compromise the model's performance at large strains: as demonstrated in the right column of Figure 4, the simulated deviatoric stress and excess pore pressure responses remain accurate, and the typical characteristics of soft clays—such as structure and overconsolidation—are well preserved. Thus, SHM provides a unified framework that captures both small-strain nonlinearity and large-strain plastic behavior without mutual interference.

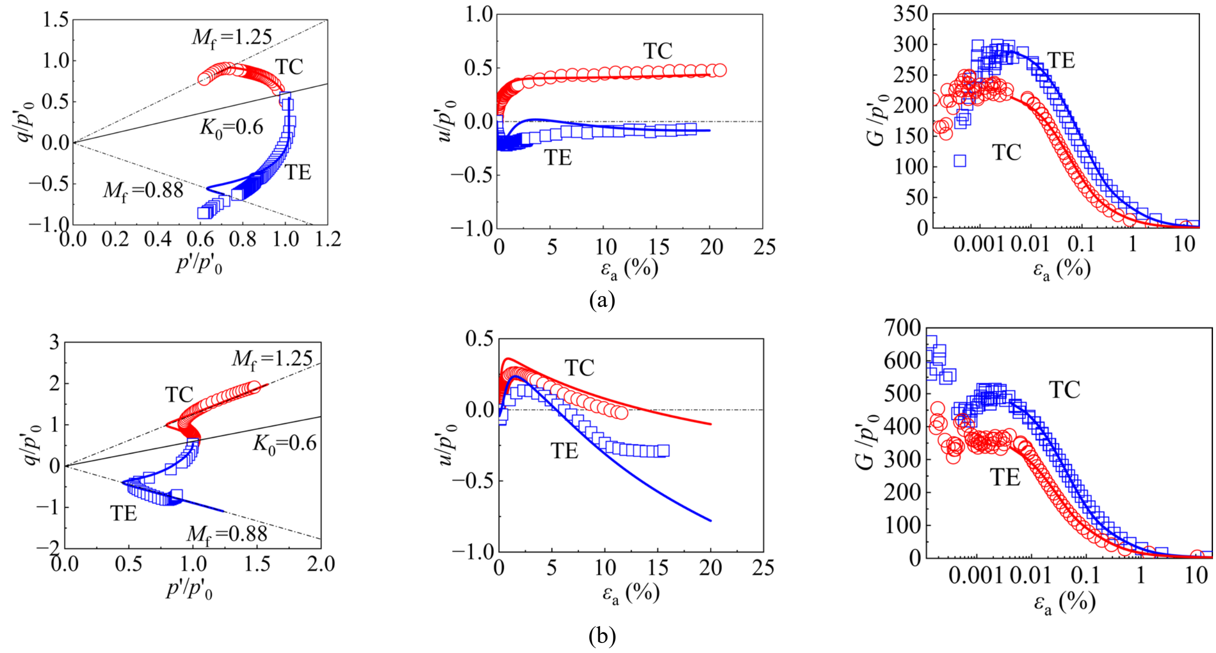

Figure 4. Typical experimental and simulated results of CK_0U tests: (a) structured clay (Layer 4) , (b) overconsolidated clay (Layer 6).

4 Conclusion

In this paper, a detailed description of newly proposed Shanghai Model (SHM) is given out. The model can comprehensively take into consideration the effects of overconsolidation, structure, anisotropy and SSS of natural deposit clays. The parameter calibration method is established and the model is validated by a series of laboratory tests. The following conclusions are drawn:

1. The newly proposed SHM is able to accurately simulate the mechanical behavior of typical Shanghai soft clays. The influence of overconsolidation, structure and anisotropy, as well as the SSS degradation are taken into consideration.
2. It is necessary to incorporate the SSS into the model and consider the initial anisotropy ζ_0 in the simulations. The incorporation of SSS does not affect the simulated results in large strain range (ε>1%) but improves significantly the performance at small-strain range (0.001%–0.1%). By proper consideration of initial anisotropy ζ_0, the model can simulate properly the asymmetric stress paths of triaxial compression/tension tests.
3. A practical procedure for parameter calibration is established with one set of parameters for various soil layers, by which SHM can reproduce various tests with different stress paths, including K_0-consolidation, triaxial compression and extension, in terms of stress-strain relationships, effective stress path, excessive pore pressure and SSS degradation.
4. The simulations and test results agree well with each and can both provide insights into the mechanical behavior of natural deposit clays under various loading conditions and internal condition of overconsolidation, structure and anisotropy.

References

1. H. Sekiguchi, Induced anisotropy and time dependency in clays, In: Constitutive equations of soils. Proc. of 9th ICSMFE, Spec Ses. (pp. 229–238) (1977)
2. K. Hashiguchi, & M. Ueno, Elastoplastic constitutive laws for granular materials, constitutive equations for soils, In S. Murayama, & A. N. Schofield (Eds.), Proc. 9th ICSMFE, Spec. Ses. 9 (pp. 73–82). Tokyo: JSSMFE (1977)
3. A. Asaoka, M. Nakano, & T. Noda, Super loading yield surface concept for the saturated structured soils, In: Proc. of fourth european conference on numerical methods in geotechnical engineering-Numge98 (pp. 232-242) (1998)
4. F. Zhang, B. Ye, T. Noda, M. Nakano, & K. Nakai, Explanation of cyclic mobility of soils: Approach by stress-induced anisotropy, Soils and Foundations, **47**(4), 635-648. (2007) https://doi.org/10.3208/sandf.47.635
5. G.L. Ye, B. Ye, Investigation of the overconsolidation and structural behavior of Shanghai clays by element testing and constitutive modeling, Underground space, **1**(1), 62-77 (2016) https://doi.org/10.1016/j.undsp.2016.08.001
6. S. Zhang, G.L. Ye, L. Zhen, M.G. Li, & C.B. Chen, Constitutive model of soft soil after considering small strain stiffness decay characteristics, Journal of Shanghai Jiao Tong University, **53**(5), 535–539. (in Chinese) (2019)
7. J.A. Santos, & A.G. Correia, Reference threshold shear strain of soil. Its application to obtain a unique strain-dependent shear modulus curve for soil. In: Proc. of 15th International Conference on Soil Mechanics and Geotechnical Engineering, (pp. 267-270). Istanbul, Turkey: ASCE. (2001)